

A MINIATURE TIME-RESOLVED RAMAN SPECTROMETER FOR IN SITU PLANETARY SURFACE EXPLORATION E. Alerstam^{1,*}, J. Blacksberg¹, Y. Maruyama¹, C. Cochrane¹, G.R. Rossman². ¹Jet Propulsion Laboratory, California Institute of Technology, 4800 Oak Grove Dr., Pasadena, CA 91109, ²California Institute of Technology, Division of Geological and Planetary Sciences, Pasadena, California 91125, *erik.alerstam@jpl.nasa.gov

Overview: We present a time-resolved Raman spectrometer (TRRS) for planetary science as a means for identification and mapping of minerals even in the presence of high background fluorescence. We report on design elements and performance of the current instrument, as well as in-progress laser developments that promise orders-of-magnitude improvement in signal-to-noise.

Introduction: Raman spectroscopy has long been a candidate for the next generation of *in situ* planetary science instruments, and several instruments are under development for both NASA [1-4] and ESA [5] targeting this purpose. Raman can be performed in concert with microscopic imaging, preserving the geological context of mineral phases. In addition to minerals, Raman can identify organic materials, and has been used in the laboratory to analyze organics, for example those present in Martian meteorites [6]. In large part due to the ability to identify both minerals and organics, Raman spectroscopy has been included on the payload for the ESA ExoMars 2018 and NASA Mars 2020 (with two Raman spectroscopic instruments [3-4]) missions. Even with these clear advantages of the Raman technique, several challenges still exist when targeting mixed phase materials with Raman spectroscopy, particularly where organics are present. Of primary concern is that fluorescence makes conventional 532 nm Raman spectroscopy of many of these samples challenging.

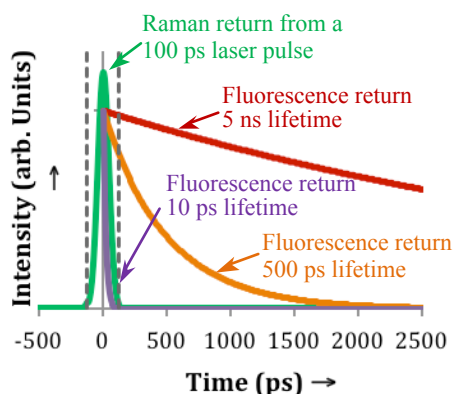


Figure 1. Illustration of the time-resolved Raman technique. The detector is only turned on (sensitive to light) during the short time when the instantaneous Raman signal arrives, as illustrated by the dashed lines. By rejecting light arriving later, all but the shortest (10 ps) lifetime fluorescence contributions are significantly reduced.

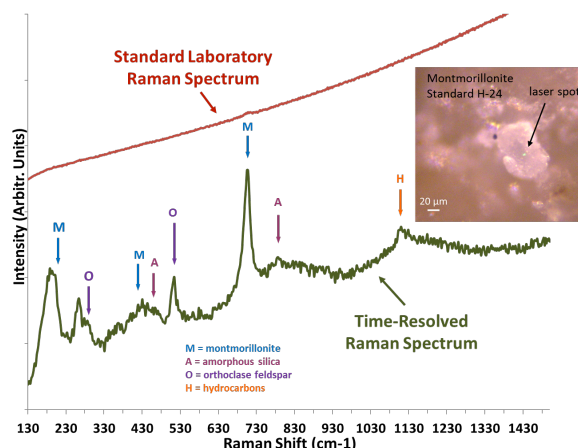


Figure 2. Illustration of the advantages of the time-resolved Raman technique. The sample is a Montmorillonite standard (H-24, Otay, California). The standard (CW excitation) laboratory Raman microscope yields little diagnostic information while a clear Raman spectrum is achieved by applying the time-resolved Raman technique.

Time-resolved Raman spectroscopy: In order to address the fluorescence problem we use the time-resolved Raman spectroscopy technique, taking advantage of the fact that fluorescence can be distinguished from Raman processes in the time domain. Raman scattering is an instantaneous process while fluorescence processes are associated with decay times which vary from ps to ms. In natural mixed-phase samples, there can be several fluorescent phases, leading to both long lifetime (mineral) and short lifetime (organic) fluorescence. An illustration of fluorescence rejection using time resolved methods is shown in Figure 1. We have developed a time-resolved Raman spectrometer that builds on the widely used 532 nm Raman technique to provide a means for performing Raman spectroscopy while minimizing the background noise that is often generated by fluorescence. An additional advantage of the time-resolved Raman technique is the rejection of interfering daylight, making daytime *in situ* measurements possible without the need for careful light shielding. Figure 2 illustrates the performance advantages of the time-resolved Raman technique over a standard continuous wave (CW) laboratory instrument.

Instrument architecture: Figure 3 shows a block diagram overview of the TRRS instrument, which is intended for potential mounting on a rover arm. A

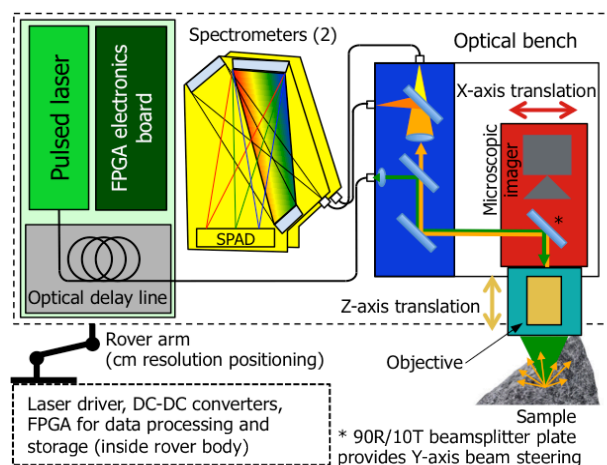


Figure 3 Block diagram of the TRRS instrument

modular design strategy is used, allowing relatively independent development and maturation of the different modules, as well as flexible placement of the modules within the instrument. The modules are optically connected using standard optical fibers. The following sections describe these key modules in more detail.

Custom time-gated detector: The heart of the instrument, and the enabling technology for a miniaturized time-resolved Raman spectroscopic instrument is the custom solid state 1024x8 Single-Photon Avalanche Diode (SPAD) detector array based on Complementary Metal-Oxide Semiconductor (CMOS) technology [7,8], shown in Figure 4. This custom chip features a high fill factor (44%), ~20% sensitivity, and is capable of sub-nanosecond time gating (down to 700 ps). Using this compact SPAD array, we have demonstrated that we can achieve equal or greater sensitivity to that achieved with traditional photocathode-based detectors such as streak cameras [9]. The use of a solid state time-resolved detector offers a significant reduction in size, weight, power, and overall complexity, putting it on par with instruments that do not have time resolution, while providing enhanced science return associated with fluorescence and daylight rejection.

Spectrometers: Currently in progress is the addition of two fiber-coupled miniature F/4 Crossed Czerny-Turner spectrometers. The two spectrometers are optimized for the -70 to 1800 cm^{-1} and 1800 to 4000 cm^{-1} spectral ranges with resolutions $<8\text{ cm}^{-1}$, and $<10\text{ cm}^{-1}$ respectively. The athermal spectrometer design is of significant flight heritage (LCROSS, LADEE, O/OREOS and MSL).

Pulsed laser: The TRRS instrument uses a commercially available miniature green (532 nm) pulsed microchip laser, generating $1.5\text{ }\mu\text{J}$, 600 ps pulses at 40 kHz repetition rate. The laser is a passively Q-switched (using a Cr:YAG saturable absorber) diode pumped (808 nm diode pumped laser) solid state (Nd:YAG) laser,

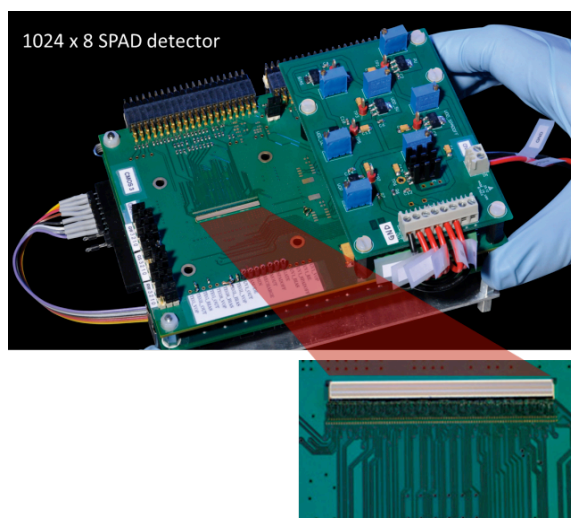


Figure 4 Custom 1024x8 SPAD array (blown up at the bottom) integrated with FPGA and power module.

operating in single mode (with the associated narrow spectral width $<0.1\text{ nm}$ and near-diffraction limited beam quality). A second harmonic generation crystal doubles the 1064 nm output to 532 nm. The laser output is coupled to a long (few meters) optical fiber, acting as an optical delay line in order to give the detector electronics time to prepare the detector gating. Using a low NA fiber ensures negligible temporal broadening of the pulse in the step-index fiber, and delivers the laser output to the optical bench.

Optical bench: The optical bench module handles delivery of the laser light to the sample ($<10\text{ }\mu\text{m}$ spot size), collection and optical filtering of the Raman-scattered light, as well as demultiplexing of the collected spectroscopic signal into two fibers connected to the two spectrometers. Furthermore, the optical bench includes a microscopic imager, providing context by imaging the sample through the same objective lens used for focusing the laser, and collecting the spectroscopic signal. This enables direct mapping of spectroscopically identified phases onto images of the surface, placing them in geological context. Finally, the optical bench includes two axis translation, as well as steering of the laser beam over the remaining axis (see Figure 3). This cm-range, μm resolution translation complements the cm-resolution positioning that would potentially be provided by a rover arm.

Advances in laser development: With the development of large format SPAD detector arrays in the past few years, time-resolved Raman spectroscopy in a miniaturized package (as described herein) has only recently been realized. The only realistic laser sources for such a miniaturized instrument have been passively Q-switched microchip lasers, offering sub-nanosecond pulses in a very small, rugged package. However, these lasers have been limited in the achievable pulse dura-

tion, pulse energy, and repetition rate, due to limitation in the passive Q-switching element: the saturable absorber (i.e., Cr:YAG crystals). In order to overcome these limitations we are developing an improved laser enabled by recent advances in semiconductor saturable absorber technology. This new class of saturable absorbers, applied as passive Q-switching elements, can be engineered to achieve a much wider variety of laser parameters, allowing us to achieve the full potential of the time-resolve Raman technique and the custom SPAD detector in a miniaturized format.

The expected improvement of TRRS with these new lasers is twofold: First, fluorescence rejection can be improved by reducing the laser pulse duration (see Figure 1). While this new technology can provide pulse durations down to 15 ps [10], we estimate that a pulse duration around 100 ps is optimal for our instrument. This improvement will lead to better rejection of fluorescence, in particular of short (sub-nanosecond) lifetime fluorescence commonly associated with organics. Second, these lasers can operate at higher repetition rates (up to several MHz) with lower pulse energies [11,12]. Lowering the pulse energy (e.g., down to a few nano-Joules) eliminates the risk of damaging or altering the samples which can occur when the pulse energy is too high (*cf.* laser-induced breakdown), while the high repetition rate ensures an appropriate average power (which is directly proportional to the measured Raman signal). The advantages of this new type of laser is illustrated in Figure 7.

Figure 8 shows a schematic overview of the new laser setup. Currently, we use a commercially available semiconductor saturable absorber mirror (SESAM) bonded to a Nd:YVO₄ laser crystal [13]. This diode pumped passively Q-switched laser setup provides 180 ps, ~15 nJ pulses (1064 nm) at 1 MHz repetition rate. Using a bulk Mg:PPLN crystal the pulses are converted to 532 nm at >30% efficiency. We are in the process of

Figure 7. SNR vs. acquisition time curves for two different samples. The curves are calculated based on measured detector noise and Raman return. (Left) For dark samples the pulse energy is limited to prevent sample damage, resulting in a clear SNR advantage for the high-rep rate laser. (Right) For a transparent sample, the pulse energy is not an issue. However, the single-photon counting operation of the custom SPAD detector limits the pulse energy to avoid detector saturation. As a result, the high-repetition rate, low pulse energy laser offers a significant SNR advantage also in this case.

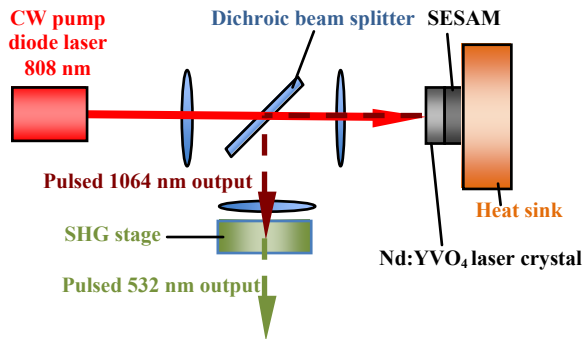
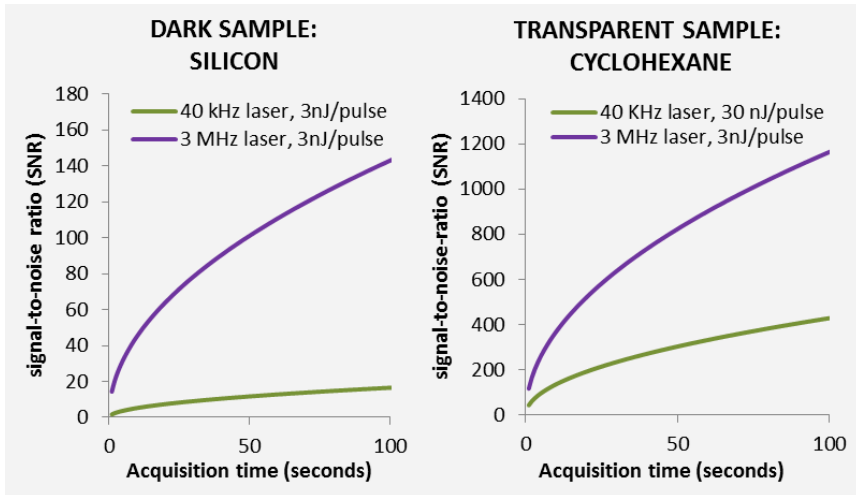


Figure 8 Schematic overview of a SESAM microchip laser illustrating the simplicity of the diode pumped, passively Q-switched laser scheme.

integrating this benchtop laser setup with our laboratory time-resolved Raman spectrometer and evaluating the performance. The next steps entail tailoring the SESAM parameters to optimize the performance for our application and working towards a miniaturized setup.

Conclusions: We present a time-resolved Raman spectrometer, capable of overcoming significant hurdles in conventional Raman spectroscopy, such as interference from fluorescence and daylight. This instrument extends the usable domain for Raman spectroscopy into environments with strong fluorescence. Recent advances in pulsed laser technology provide a path for substantial improvements in instrument performance, by overcoming limitations set by standard passive Q-switching elements. Due to our instrument’s modular design, the improved laser can potentially be substituted as a drop in replacement, offering the possibility of orders of magnitude improvements in signal-to-noise ratio, after optimization.

Acknowledgement: The research described here was carried out at the Jet Propulsion Laboratory, California Institute of Technology, under a contract with

the National Aeronautics and Space Administration (NASA). Continuous-wave Raman measurements were performed at the Mineral Spectroscopy Laboratory at the California Institute of Technology. SPAD development was performed at Delft University of Technology by the group of Professor Edoardo Charbon.

References: [1] A. Wang, et al. *J. Geophys. Res.*, 108 (E1), 5005 (2003) [2] S.K. Sharma et al. *Spectrochim. Acta Part A*, 68, 1036-1045 (2007) [3] L.W. Beegle et al., GeoRaman 2014 #5101 [4] S.M. Clegg et al., GeoRaman 2014 #5082 [5] F. Rull, et. al., LPSC 2011 #2400 [6] A. Steele et al., *Science*, 337 (6091), 212-215 (2012) [7] J. Blacksberg et al. *Optics Letters*, 36 (18), 3672-3674 (2011) [8] Y. Maruyama et al., *IEEE JSSC*, 49 (1) (2014) [9] J. Blacksberg et al., *Applied Optics*, 49 (26), 4951-4962 (2010) [10] B. Bernard et al., Proc. of SPIE Vol. 8960 (2014) [11] E. Mehner et al. *Appl. Phys. B*, 112, 231-239 (2013) [12] A. Steinmetz et al. *Appl. Phys. B*, 97, 317-320 (2009) [13] <http://www.batop.de>